

Published in final edited form as:

*J Surg Res.* 2010 June 1; 161(1): 1–8. doi:10.1016/j.jss.2009.07.028.

## Mesenteric Nitric Oxide and Superoxide Production in Experimental Necrotizing Enterocolitis

Jill S. Whitehouse, M.D.<sup>\*,†</sup>, Hao Xu, Ph.D.<sup>\*,‡,†</sup>, Yang Shi, Ph.D.<sup>\*,‡,†</sup>, LeAnne Noll, B.S.<sup>\*</sup>, Sushma Kaul, M.S.<sup>\*,†,‡</sup>, Deron W. Jones, B.S.<sup>\*,†,‡</sup>, Kirkwood A. Pritchard Jr., Ph.D.<sup>\*,‡,†</sup>, Keith T. Oldham, M.D.<sup>\*,†,‡</sup>, and David M. Gourlay, M.D.<sup>\*,†,‡,1</sup>

<sup>\*</sup>Medical College of Wisconsin, Milwaukee, Wisconsin

<sup>†</sup>Children's Research Institute, Milwaukee, Wisconsin

<sup>‡</sup>Division of Pediatric Surgery, Milwaukee, Wisconsin

### Abstract

**Background**—A proposed mechanism of intestinal injury in necrotizing enterocolitis (NEC) involves vascular dysfunction through altered nitric oxide synthase (NOS) activity. We hypothesize that this dysfunction results in an imbalance in nitric oxide ( $\bullet\text{NO}$ ) and superoxide ( $\text{O}_2^{\bullet-}$ ) production by the intestinal vascular endothelium, which contributes to the intestinal injury seen in NEC.

**Materials and Methods**—Neonatal rat pups were divided into two groups. Control pups were breast fed and housed with their mother. Experimental NEC pups were housed separately and either exposed to formula feeding and 5% to 10% hypoxia alone (FF/H) or with the addition of lipopolysaccharide (FF/H/LPS). Mesenteries from each group were analyzed for  $\bullet\text{NO}$  and  $\text{O}_2^{\bullet-}$  production with and without NOS inhibition by  $\text{N}^G$ -monomethyl-L-arginine (L-NMMA). Western blot analysis for eNOS, phosphorylated eNOS (phospho-eNOS), and inducible NOS (iNOS) was performed, and each terminal ileum was graded for intestinal injury by histology.

**Results**—Histology revealed mild intestinal injury (grade 1–2 on a 4-point scale) in the FF/H group and severe injury (grade 3–4) in the FF/H/LPS group. The FF/H cohort had significantly increased  $\bullet\text{NO}$  and lower  $\text{O}_2^{\bullet-}$  production, while the FF/H/LPS group shifted to significantly decreased  $\bullet\text{NO}$  and increased  $\text{O}_2^{\bullet-}$  production. L-NMMA inhibited >50% of  $\text{O}_2^{\bullet-}$  production in all three groups but only inhibited  $\bullet\text{NO}$  production in control and FF/H pups. Western blot analysis revealed increased levels of phospho-eNOS in FF/H pups and increased iNOS in FF/H/LPS pups.

**Conclusions**—This study demonstrates in the progression of NEC, intestinal ischemia is associated with a shift from  $\bullet\text{NO}$  to  $\text{O}_2^{\bullet-}$  production, which is NOS-dependent. Potentially greater injury results from impaired vasodilatation and over-production of reactive oxygen species.

### Keywords

necrotizing enterocolitis; nitric oxide; superoxide; nitric oxide synthase; uncoupled nitric oxide synthase; lipopolysaccharide

## INTRODUCTION

Necrotizing enterocolitis (NEC) causes significant morbidity and mortality in neonates. NEC occurs at a frequency of 0.3 to 2.4 per 1000 live births, and 70% of the cases occur in infants born <36 wk gestational age [1]. More specifically, premature infants with birth weights <1500 g (very low birth weight, VLBW) are at the greatest risk and account for 70% to 90% of all cases with NEC [1, 2]. NEC is the most common surgical emergency in neonatal intensive care units (NICU), and mortality rates are as high as 50% [1, 3, 4].

A significant amount of research over the past four decades has focused on the microvascular, cellular and molecular mechanisms mediating NEC. A variety of components have been implicated, including inflammatory markers, gut barrier function, vascular dysfunction, and infectious complications [3, 5–8]. Several reports suggest that alterations in nitric oxide ( $\bullet$ NO) production are involved in the development of intestinal ischemia [5, 6, 9, 10]. Emerging evidence indicates that coronary ischemia, diabetes mellitus, hyperlipidemia, and pulmonary hypertension all induce endothelial nitric oxide synthase (eNOS) to switch from producing  $\bullet$ NO to superoxide ( $O_2^{\bullet-}$ ) [11–14]. When eNOS generates  $O_2^{\bullet-}$  rather than  $\bullet$ NO, this switch in enzyme function is called “eNOS uncoupling.” All NOS isoforms, however, are capable of becoming uncoupled when deprived of essential cofactors, suggesting that eNOS may not be the only source of an imbalance of  $\bullet$ NO and  $O_2^{\bullet-}$  production [15–17]. The other isoforms include neuronal NOS (nNOS), which is constitutively expressed like eNOS, and inducible NOS (iNOS), which is expressed in the setting of inflammation, stress, or sepsis and is calcium-independent [5, 16].

We hypothesize that NOS uncoupling in the intestinal vascular endothelium occurs in NEC, leading to a shift in vascular function that switches from a protective vasodilatory state to a vasoconstrictive state and increased generation of reactive oxygen species. To test this hypothesis, we examined changes in  $\bullet$ NO and  $O_2^{\bullet-}$  generation in neonatal rat intestinal mesenteries during all phases of experimental NEC.

## METHODS

### Animal Model

All animal protocols were approved by the Institutional Animal Care and Use Committee and followed a well-described neonatal rat model of NEC [7, 8, 18–20]. Litters of full-term Sprague-Dawley rat pups (Harlan Laboratories, Madison, WI) were split into two groups several hours after birth. Control pups remained with the mother, were breast fed, and kept at normoxia and normothermia. The experimental pups were housed separately from the mother in an Air-Shields T-100 infant transport incubator (Soma Technologies, Bloomfield, CT) set at 37 °C. They were exposed to hypoxia by placing them in a room temperature Praxair Biosperix chamber, (Lacona, NY) and subjected to 5%–10% oxygen for 10 min, 3 times daily. This range in hypoxia was due to fluctuating levels within the chamber when the door was opened to place the animals inside. Additionally, they were gavage-fed transorally with formula three times per day using a 24-gauge blunt-tipped angiocatheter (Instech Solomon, Plymouth Meeting, PA). Neonatal rats were fed a combination of Similac infant formula (15 g; Abbott Laboratories, Columbus, OH) in Esbilac canine milk replacement (75 mL; PetAg Inc., Hampshire, IL) [7]. The pups exposed to formula feeding and intermittent hypoxia (FF/H) were used to induce an early, less severe stage of experimental NEC. Additional pups were also exposed to 2 mg/kg enteral lipopolysaccharide (LPS from *Escherichia coli*; Sigma-Aldrich) to induce a later, more severe injury (FF/H/LPS). A total of 0.2 mL was fed to each pup per feeding.

The pups were sacrificed on days 2–5 after birth using intraperitoneal injections of pentobarbital (60–80 mg/kg). Laparotomies were performed and the entire intestinal tract from the distal esophagus to distal rectum was removed. First, a short segment of terminal ileum was harvested for histology grading of NEC. Tissues were fixed in zinc formalin (Richard-Allan Scientific, Kalamazoo, MI) processed, and subsequently embedded in paraffin. Hematoxylin and eosin staining was performed on 4  $\mu$  thick sections. Tissues were graded using a four-point scale as described by Nadler (Table 1) [7]. Second, the entire intestinal mesentery from the duodenum to rectum was carefully dissected from the bowel. This tissue was placed in fresh Hanks balanced salt solution (HBSS; Sigma-Aldrich) on ice and subsequently used for  $\bullet$ NO and  $O_2^{\bullet-}$  analysis as well as for Western blot analysis to detect eNOS, phosphorylated eNOS (phospho-eNOS, S1179), and iNOS.

### Nitric Oxide Analysis

Isolated mesenteries were suspended in 250  $\mu$ L of fresh HBSS containing 25  $\mu$ M L-arginine (Sigma-Aldrich) and incubated for 30 min at 37  $^{\circ}$ C. Following incubation, 150  $\mu$ L of the supernatant was removed and saved for  $\bullet$ NO analysis. Next, 100  $\mu$ L of 10  $\mu$ M A23187 (Calbiochem, San Diego, CA) was added to the original sample and again incubated for 30 min at 37  $^{\circ}$ C, yielding a final A23187 concentration of 5  $\mu$ M. A23187 is a calcium ionophore that stimulates constitutive isoforms of NOS by elevating intracellular calcium levels. Increased intracellular calcium subsequently stimulates the binding of calmodulin to both eNOS and neuronal NOS (nNOS), which is an essential step in NOS activation [16, 21, 22]. Since iNOS is calcium-independent, A23187 should not lead to further stimulation of  $\bullet$ NO production by this isoform. To test the effects of NOS inhibition, some of the mesenteries were also incubated with 250  $\mu$ M  $N^G$ -monomethyl-L-arginine (L-NMMA; Alexis Biochemicals, Plymouth Meeting, PA) for 30 min. L-NMMA is an arginine analog that blocks arginine access to the active site of NOS, therefore blocking  $\bullet$ NO production [22]. One hundred fifty  $\mu$ L of the supernatant was removed for  $\bullet$ NO analysis. Both samples from each mesentery were then analyzed for  $\bullet$ NO content by injecting 25  $\mu$ L into a Sievers 280i  $\bullet$ NO analyzer (Boulder, CO) containing vanadium chloride, as described in the manual.  $\bullet$ NO concentrations in the samples were compared with known nitrate standards ranging from 0 to 10  $\mu$ M, and findings were normalized to tissue protein. Values were expressed in nmol/mg protein to account for variation in the amount of protein harvested from each mesentery.

### Superoxide Anion Analysis

Mesenteries were placed in HBSS (500  $\mu$ L) in a 1.5 mL microcentrifuge tube. The tubes were placed into a Turner 20/20 luminometer (Turner Biosystems, Sunnyvale, CA) in a dark room to measure luminescence. A luminescent  $O_2^{\bullet-}$  detecting reagent, L012 (Wako Pure Chemical, Osaka, Japan), was added to each tube at a final concentration of 200  $\mu$ M and incubated for 5 min. Next, luminescence (relative light units, RLU) was recorded dynamically every second for 5 min. The microfuge tube was removed, A23187 added (final concentration, 5  $\mu$ M), and luminescence recorded again for 5 min. NOS inhibition was performed by incubating the mesenteries with 1 mM L-NMMA. Mesenteries were washed twice with phosphate buffered saline (PBS; Sigma-Aldrich) and saved for protein determination. Rates of  $O_2^{\bullet-}$  production were normalized to tissue protein and expressed as RLU/mg protein/min.

### Protein Quantification and Western Blot Analysis

Neonatal rat mesenteries were placed in fresh HBSS (500  $\mu$ L) in a 2 mL microfuge tube (Axygen Scientific, Union City, CA). The mesenteries were cut into small pieces using alcohol-treated fine scissors and homogenized while on ice (3 bursts, 10 s each burst) using a hand-held Polytron PT 1200 E homogenizer (Kinematica, Inc., Bohemia, NY).

Homogenates were lysed with MOPS buffer [23] (500  $\mu$ L) containing protease and phosphatase inhibitors (Sigma-Aldrich). The tubes were centrifuged at 14,000 rpm for 10 min at 4  $^{\circ}$ C to pellet cell debris. The supernatant was removed and saved for both protein quantification and Western blot analysis. Protein content was quantified using the bicinchoninic acid (BCA) reagent per the manufacturer's protocol (Pierce Chemical Company, Rockford, IL).

Equal volumes of 5  $\times$  Laemmli sample buffer (Bio-Rad, Hercules, CA) were added to each protein sample. MOPS lysis buffer was used to bring the total volume to 100  $\mu$ L. Samples were heated at 95  $^{\circ}$ C for 5 min, cooled to room temperature (RT), and then loaded onto a 4% to 15% Tris-HCl Criterion gel system (Bio-Rad). Tris-Glycine SDS running buffer was used as well as All Blue and Dual Rainbow markers (Bio-Rad). Protein was transferred to a 0.45  $\mu$  nitrocellulose membrane using the Criterion blotting system (4  $^{\circ}$ C, 55 V for 2 h, Bio-Rad). The membrane was incubated for 1 h at room temperature in TBS-T blocking buffer containing 5% non-fat dry milk (SantaCruz Biotechnologies, Santa Cruz, CA). Primary antibodies were a rabbit, polyclonal anti-eNOS antibody (1:1000) (NOS-3, Santa Cruz Biotechnologies), rabbit, polyclonal anti-phospho-eNOS (S1179) antibody (1:1000) (Cell Signaling Technology, Danvers, MA), rabbit, polyclonal anti-iNOS antibody (1:1000, Santa Cruz Biotechnologies), and mouse, monoclonal anti- $\beta$ -actin antibody to control for loading (1:1000) (Santa Cruz Biotechnologies). Incubations were in PBS-T containing 5% BSA (Sigma-Aldrich). The membranes were incubated overnight at 4  $^{\circ}$ C on an orbital shaker. The next morning membranes were washed with TBS-T and then incubated with the appropriate secondary antibodies [goat anti-rabbit IgG HRP and goat anti-mouse IgG HRP (1:5000 from Santa Cruz Biotechnologies)] for 1 h at RT. The membranes were washed with TBS-T. Bands of identity were detected using ECL Plus and Hyper-film ECL according to the manufacturer's instructions (Amersham/GE Healthcare, Piscataway, NJ).

### Statistical Analysis

Computerized densitometry of the film using UN-SCAN-IT software (version 6.1, Silk Scientific, Inc., Orem, UT) was used to capture bands and quantify differences in band intensities in the autoradiograms. Statistical analysis was performed using the Student's *t*-test with  $P \leq 0.05$  set as being significant.

## RESULTS

Fourteen litters with an average of 13 pups/litter were used for the studies. Out of a total of 191 pups, 22 died before analysis could be completed, resulting in a total of 171 pups that underwent analysis (Table 2). The peak NEC grade observed in surviving FF/H pups was 2 (median = 1), while those in the FF/H/LPS group demonstrated a peak grade of 4 (median = 2) (Fig. 1).

Although increased production of  $\bullet$ NO by the intestinal mucosa appears to contribute to NEC, previous research has suggested that endothelial  $\bullet$ NO production is decreased after intestinal necrosis has occurred [18]. We questioned whether there is impaired endothelial production of  $\bullet$ NO and, if so, when does it occur during the development of NEC. To answer this question, we isolated the intestinal mesentery from the animals to measure  $\bullet$ NO production. To study an early, potentially reversible phase of intestinal injury, the FF/H pups were sacrificed earlier, on day of life 2–3. To study a late phase of NEC we added LPS to the formula of the FF/H/LPS pups and animals were sacrificed on day of life 4–5. These results are presented graphically in Fig. 2. At baseline, the mesenteries from control pups generated  $\bullet$ NO at an average of 2.066 nmol/mg protein. Interestingly, A23187 stimulation of these vessels did not significantly increase  $\bullet$ NO production (2.359 nmol/mg protein,  $P = 0.35$ ).  $\bullet$ NO production by mesenteries from FF/H pups at baseline (6.252 nmol/mg protein)

and after A23187 stimulation (6.416 nmol/mg protein) was significantly increased compared with the levels of •NO production by mesenteries isolated from controls ( $P \leq 0.01$ ). Similarly, no significant differences in •NO production were observed when mesenteries from FF/H pups were stimulated with A23187 ( $P = 0.47$ ). The FF/H/LPS pups, however, had significantly decreased •NO production both at baseline (0.981 nmol/mg protein) and after A23187 stimulation (0.651 nmol/mg protein) compared with controls and FF/H pups ( $P < 0.05$ ).

To determine if the differences in •NO production were mediated by NOS, we repeated the above assays in the presence of L-NMMA. In the control pups, 78.8% and 90.9% of the •NO signal was inhibited at baseline and following A23187 stimulation, respectively. Greater than 98% of •NO signal in the FF/H pups was inhibited both at baseline and following A23187 stimulation. These data suggest that the source of •NO in these mesenteries is NOS-dependent. Interestingly, further stimulation with A23187 did not significantly increase •NO production. The small amount of •NO that was produced in the FF/H/LPS pups was not inhibited by L-NMMA.

Next, we questioned whether the intestinal mesentery was producing excessive  $O_2^{\bullet-}$  instead of •NO.  $O_2^{\bullet-}$  production was determined in mesenteries isolated from five different litters (Fig. 3). At baseline,  $O_2^{\bullet-}$  production tended to decrease in the FF/H group compared with control pups, but did not achieve statistical significance (185,909 versus 96,552 RLU/mg protein/min,  $P = 0.09$ ) because of increased variation. After stimulation with A23187, however, the stimulated  $O_2^{\bullet-}$  production was much lower in the FF/H compared with the controls (307,918 versus 175,227 RLU/mg protein/min,  $P = 0.01$ ). The FF/H/LPS treated pups produced significantly more  $O_2^{\bullet-}$  both at baseline (282,310 RLU/mg protein/min) and following stimulation (760,001 RLU/mg protein/min) compared with the control and FF/H cohorts ( $P < 0.05$ ). Similar to our •NO data, the addition of L-NMMA to the mesenteries inhibited virtually all of the  $O_2^{\bullet-}$  produced in control pups both at baseline and after A23187 stimulation (99.3% and 94.1%, respectively). In the FF/H group, however, 72.2% of the  $O_2^{\bullet-}$  production at baseline and only 53.2% following A23187 stimulation was inhibited by L-NMMA, suggesting that early in the disease progression when NOS dependent •NO production is at its peak,  $O_2^{\bullet-}$  may be generated from different oxidative enzyme sources. Later, in the FF/H/LPS group,  $O_2^{\bullet-}$  production is significantly inhibited by L-NMMA both at baseline and after A23187 stimulation (94% and 89.4%, respectively). This indicates a significant change in NOS function where the enzyme preferentially generates  $O_2^{\bullet-}$  instead of •NO. The fact that L-NMMA inhibited  $O_2^{\bullet-}$  production confirms that it is NOS-dependent.

It has been suggested that endothelial dysfunction occurs as the result of impaired eNOS function [1, 11, 12, 24]. Therefore, we measured total eNOS and phospho-eNOS, to assess eNOS expression and activation, from the intestinal mesentery from control, FF/H, and FF/H/LPS pups (Fig. 4). Equal protein loading was confirmed by probing for  $\beta$ -actin (data not shown) and densitometry measurements were recorded to quantify the amount of protein detected. All samples contained similar amounts of total eNOS, but those from the FF/H group had significantly more phospho-eNOS compared with both control and FF/H/LPS groups ( $P < 0.05$ ). These data are consistent with the •NO data showing that mesenteries isolated from the FF/H NEC pups generate more •NO than mesenteries from control pups. We did not observe an increase in phospho-eNOS in the FF/H/LPS group compared with the control pups, which correlates to decreased •NO production in this group.

Since increased expression of iNOS is known to occur in the intestinal mucosa during the development of NEC and is a potential source for production of reactive oxygen species, we investigated this as well. The Western blot analysis and densitometry data for iNOS from



protein extracts of the rat mesentery are shown in Fig. 5. Neither control or FF/H samples contain significant levels of iNOS, but a significant increase in iNOS was observed in the FF/H/LPS samples compared with controls ( $P < 0.05$ ), indicating that iNOS was increased in the intestinal mesentery in late NEC.

## DISCUSSION

To date, much of what we understand about the cellular biology of NEC is from end-stage NEC, after necrosis has occurred. The purpose of this study was to examine intestinal endothelial function throughout the progression of NEC in order to identify potentially reversible stages of the disease. We believe that premature infants are predisposed to intestinal ischemic injury due, at least in part, to repeated episodes of stressful stimulation. If true, and if the effects of repeated stress at a cellular level are understood, we may be able to develop new means of preventing NEC. To investigate cellular mechanisms, we used a model of NEC first developed by Barlow [8, 20] and subsequently modified to include additional experimental factors [7, 19]. We chose to induce early NEC using similar methods of intermittent hypoxia and gavage formula feeding to mimic human disease. In contrast to what has been done by others, we sacrificed these pups on day 2 or 3 after birth, so that we could observe changes during very early stages of the disease, and did not use tissue from animals that had developed intestinal necrosis. As demonstrated, these animals had only mild intestinal injury. Focusing on the early stages in the rodent model of NEC allowed us to examine vascular and cellular changes occurring prior to irreversible bowel necrosis and/or perforation. To study the progression of the vascular dysfunction, a later stage of NEC was induced by adding LPS to the formula and allowing the disease to progress until day of life 4–5. Our data demonstrate that these animals had significantly more intestinal injury than the FF/H group and allowed us to examine a later stage in the pathogenesis of NEC.

We were particularly interested in the role of vascular dysfunction in the development of NEC. Although endothelial dysfunction has been well studied in other ischemic disease processes and the role of  $\bullet\text{NO}$  in NEC has been studied in both human tissue and animal models, findings are sometimes conflicting [5, 7, 11, 12, 18]. Furthermore, the deleterious effects of  $\text{O}_2^{\bullet-}$  production in NEC and other pathologic conditions has also been well studied, but the precise cause of the imbalance of  $\bullet\text{NO}$  and  $\text{O}_2^{\bullet-}$  production is unclear [24, 25]. Our data suggest an increase in  $\bullet\text{NO}$  and a decrease in  $\text{O}_2^{\bullet-}$  production occur in early NEC, which presumably is a compensatory mechanism to preserve mesenteric blood flow during periods of hypoxia and inflammation. Subsequently,  $\bullet\text{NO}$  production decreased significantly, which parallels a prior report by Nowicki *et al.* who showed that arterioles isolated from infants with NEC exhibited impaired vasodilatation compared with control infants with congenital bowel malformations [18].

It is still unclear as to which NOS isoform plays the most significant role in the intestinal mesentery. We did not examine nNOS in this study because our focus was on the vascular dysfunction. Similar to our study, Ford *et al.* found increased  $\bullet\text{NO}$  production in tissue specimens from infants with NEC. However, they attributed the increase to an up-regulation of inducible NOS (iNOS) within the intestinal epithelium [5]. Similarly, in an experimental rat model of NEC, iNOS and  $\bullet\text{NO}$  production were observed to be increased [7]. Although we were able to demonstrate increased iNOS expression in the intestinal mesentery in late NEC, this was associated with increased  $\text{O}_2^{\bullet-}$  rather than  $\bullet\text{NO}$  production by the mesentery. The total amount of eNOS did not change in the pups, but activation as assessed by eNOS phosphorylation initially increased in early NEC and then returned to control levels in late NEC coinciding with the changes in NO production [29]. These findings suggest that eNOS may play a larger role in the initial rise in  $\bullet\text{NO}$  production, but then a combination of

uncoupled eNOS and iNOS activity takes over to account for the subsequent increase in L-NMMA-inhibitable  $O_2^{\bullet-}$  production. This shift towards NOS-dependent reactive oxygen species generation is hypothesized to lead to a hypervasoconstricted state, likely contributing to the severe ischemia associated with late stage NEC.

Interestingly, our data demonstrate there is a reciprocal relationship between NOS-dependent  $\bullet NO$  and  $O_2^{\bullet-}$  production in the mesentery of NEC pups. While others report decreased eNOS activity and decreased  $\bullet NO$  production by intestinal vasculature during NEC, we believe that our data could support the alternative mechanism that NOS is actually active but uncoupled. The mechanisms governing uncoupled NOS activity require further exploration and are the subject of future experiments.

Although we conclude the increase in  $O_2^{\bullet-}$  production in severe NEC is from uncoupled NOS activity, alternate explanations are possible. One explanation for an imbalance in  $\bullet NO$  and  $O_2^{\bullet-}$  production in NEC is differences in  $O_2^{\bullet-}$  metabolism and antioxidant enzyme expression, which we did not examine. One report in rats with experimental NEC found increased levels of superoxide dismutase (SOD) in neonatal tissue [25], which should be protective. We know that  $O_2^{\bullet-}$  can be generated by multiple oxidative enzymes, including NADPH oxidase, mitochondrial oxidase, xanthine oxidase, and cyclooxygenase [26, 27]. Once generated,  $O_2^{\bullet-}$  can react with  $\bullet NO$  to form peroxynitrite or be dismutated by SOD to form hydrogen peroxide. These products can then enter any one of a number of pathways, some of which produce additional reactive oxygen species that can exaggerate NOS uncoupling [26, 28]. The most compelling data supporting uncoupled NOS activity is a decrease in  $O_2^{\bullet-}$  production when NOS was inhibited with L-NMMA. Thus, despite potential multiple sources of  $O_2^{\bullet-}$  production, it appears that uncoupled NOS activity plays an important role in this experimental model of NEC.

There are several limitations to this study. First, the precise mechanism responsible for the shift toward reactive oxygen species production remains to be determined. Future directions include studying the role of critical cofactors that promote NOS uncoupling. These include  $BH_4$ , L-arginine, and heat shock protein 90 (hsp 90) [11, 17, 23, 24, 30]. Additionally, alternate sources of  $O_2^{\bullet-}$ , such as NADPH oxidase and/or xanthine oxidase, should be examined to determine the extent to which each oxidation enzyme plays a role in the  $\bullet NO$  and  $O_2^{\bullet-}$  imbalance. Finally, we studied intact mesenteries, which limit our ability to implicate a specific cell type in the progression of NEC. Although we believe that endothelial dysfunction plays an important role in the intestinal injury, further studies are needed to elucidate the cellular mechanism. One way we plan to address this limitation is to harvest human intestinal microvascular endothelial cells (HIMECs) [31] from infants undergoing bowel resection for NEC or congenital malformations. Such cells will allow us to investigate potential mechanisms of vascular dysfunction in NEC at the cellular level, and correlate findings using human cells with findings from our animal model.

In conclusion, throughout the progression of NEC, mesenteric  $\bullet NO$  production initially increases, which we believe helps protect the intestinal blood flow *via* increasing vasodilation, but as NOS becomes uncoupled in states of chronic inflammation and oxidative stress, this also contributes to a shift in NOS-dependent  $O_2^{\bullet-}$  production. In late stages of NEC, mesenteric  $\bullet NO$  production decreases and  $O_2^{\bullet-}$  production increases. Our results indicate that the reciprocal changes in  $\bullet NO$  and  $O_2^{\bullet-}$  production by the mesenteric vasculature are NOS-dependent and suggest that NOS uncoupling becomes worse during the progression through the pathogenesis of NEC. When imbalances favor reactive oxygen species, this likely contributes to vasoconstriction, and, ultimately, intestinal ischemia. Understanding the cellular mechanisms driving this imbalance may lead to the design of

therapeutic strategies to protect neonatal intestinal vasculature and thus reduce the morbidity and mortality associated with NEC.

## Acknowledgments

The authors thank David Purpi and Kevin Riggle for their technical assistance with the animal model, Dr. Suresh Kumar for his assistance with histology imaging, and the core histology lab for sectioning and staining the rat intestinal tissue.

## REFERENCES

- Hunter CJ, Upperman JS, Ford HR, et al. Understanding the susceptibility of the premature infant to necrotizing enterocolitis (NEC). *Pediatr Res*. 2008; 63:117. [PubMed: 18091350]
- Schnabl KL, VanAerde JE, Thomson ABR, et al. Necrotizing enterocolitis: A multifactorial disease with no cure. *World J Gastroenterol*. 2008; 14:2142. [PubMed: 18407587]
- Lin PW, Nasr TR, Stoll BJ. Necrotizing enterocolitis: Recent scientific advances in pathophysiology and prevention. *Semin Perinatol*. 2008; 32:70. [PubMed: 18346530]
- Ladd AP, Rescorla FJ, West KW, et al. Long-term follow-up after bowel resection for necrotizing enterocolitis: Factors affecting outcome. *J Pediatr Surg*. 1998; 33:967. [PubMed: 9694079]
- Ford H, Watkins S, Reblock K, et al. The role of inflammatory cytokines and nitric oxide in the pathogenesis of necrotizing enterocolitis. *J Pediatr Surg*. 1997; 32:275. [PubMed: 9044137]
- Nankervis CA, Giannone PJ, Reber KM. The neonatal intestinal vasculature: Contributing factors to necrotizing enterocolitis. *Semin Perinatol*. 2008; 32:83.
- Nadler EP, Dickinson E, Knisely A, et al. Expression of inducible nitric oxide synthase and interleukin-12 in experimental necrotizing enterocolitis. *J Surg Res*. 2000; 92:71. [PubMed: 10864485]
- Barlow B, Santulli TV. Importance of multiple episodes of hypoxia or cold stress on the development of enterocolitis in an animal model. *Surgery*. 1975; 77:687. [PubMed: 1173200]
- Potoka DA, Nadler EP, Upperman JS, et al. Role of nitric oxide and peroxynitrite in gut barrier failure. *World J Surg*. 2002; 26:806. [PubMed: 11948371]
- Upperman JS, Potoka DA, Grishin A, et al. Mechanism of nitric oxide-mediated intestinal barrier function in necrotizing enterocolitis. *Semin Pediatr Surg*. 2005; 14:159. [PubMed: 16084403]
- Alp NJ, Mussa S, Khoo J, et al. Tetrahydrobiopterin-dependent preservation of nitric-oxide-mediated endothelial function in diabetes by targeted transgenic GTP-cyclohydrolase I overexpression. *J Clin Invest*. 2003; 112:725-12.
- Dumitrescu C, Biondi R, Xia Y, et al. Myocardial ischemia results in tetrahydrobiopterin (BH<sub>4</sub>) oxidation with impaired endothelial function ameliorated by BH<sub>4</sub>. *Proc Natl Acad Sci USA*. 2007; 104:15081. [PubMed: 17848522]
- Molhau H, Schulz E, Daiber A, et al. Nebivolol prevents vascular NOS III uncoupling in experimental hyperlipidemia and inhibits NADPH oxidase activity in inflammatory cells. *Arterioscler Thromb Vasc Biol*. 2003; 23:615. [PubMed: 12692005]
- Pritchard KA Jr, Groszek L, Smalley DM, et al. Native low-density lipoprotein increases endothelial cell nitric oxide synthase generation of superoxide anion. *Circ Res*. 1995; 77:510. [PubMed: 7543827]
- Pall ML. Nitric oxide synthase partial uncoupling as a key switching mechanism for the NO/ONOO<sup>-</sup> cycle. *Med Hypotheses*. 2007; 69:821. [PubMed: 17448611]
- Andrew PJ, Mayer B. Enzymatic function of nitric oxide synthases. *Cardiovasc Res*. 1999; 43:521. [PubMed: 10690324]
- Chokshi NK, Guner YS, Hunter CJ, et al. The role of nitric oxide in intestinal epithelial injury and restitution in neonatal necrotizing enterocolitis. *Semin Perinatol*. 2008; 32:92. [PubMed: 18346532]
- Nowicki PT, Caniano DA, Hammond S, et al. Endothelial nitric oxide synthase in human intestine resected for necrotizing enterocolitis. *J Pediatr*. 2007; 150:40. [PubMed: 17188611]



19. Dvorak B, Halpern MD, Holubec H, et al. Epidermal growth factor reduces the development of necrotizing enterocolitis in a neonatal rat model. *Am J Physiol Gastrointest Liver Physiol.* 2002; 282:156.
20. Barlow B, Santulli TV, Heird WC, et al. An experimental study of acute neonatal enterocolitis—the importance of breast milk. *J Pediatr Surg.* 1974; 9:587. [PubMed: 4138917]
21. Bolander FF Jr. Prolactin activation of mammary nitric oxide synthase: Molecular mechanisms. *J Mol Endocrinol.* 2002; 28:45. [PubMed: 11854098]
22. Southan GJ, Szabo C. Selective pharmacological inhibition of distinct nitric oxide synthase isoforms. *Biochem Pharmacol.* 1996; 51:383. [PubMed: 8619882]
23. Xu H, Shi Y, Wang J, et al. A heat shock protein 90 binding domain in endothelial nitric oxide synthase influences enzyme function. *J Biol Chem.* 2007; 282:37567. [PubMed: 17971446]
24. Munzel T, Sinning C, Post F, et al. Pathophysiology, diagnosis and prognostic implications of endothelial dysfunction. *Ann Med.* 2008; 40:180. [PubMed: 18382884]
25. Chan KL, Hui CWC, Chan KW, et al. Revisiting ischemia and reperfusion injury as a possible cause of necrotizing enterocolitis: Role of nitric oxide and superoxide dismutase. *J Pediatr Surg.* 2002; 37:828. [PubMed: 12037744]
26. Miller AA, Drummond GR, Sobey CG. Reactive oxygen species in the cerebral circulation: Are they all bad? *Antioxid Redox Signal.* 2006; 8:1113. [PubMed: 16910759]
27. Guzik TJ, Mussa S, Gastaldi D, et al. Mechanisms of increased vascular superoxide production in human diabetes mellitus: Role of NAD(P)H oxidase and endothelial nitric oxide synthase. *Circulation.* 2002; 105:1656. [PubMed: 11940543]
28. Chen C, Druhan LJ, Varadharaj S, et al. Phosphorylation of endothelial nitric-oxide synthase regulates superoxide generation from the enzyme. *J Biol Chem.* 2008; 282:27038. [PubMed: 18622039]
29. Dimmeler S, Fleming I, Fisslthaler B, et al. Activation of nitric oxide synthase in endothelial cells by Akt-dependent phosphorylation. *Nature.* 1999; 399:601. [PubMed: 10376603]
30. Amin HG, Zamora SA, McMillan DD, et al. Arginine supplementation prevents necrotizing enterocolitis in the premature infant. *J Pediatr.* 2002; 140:425. [PubMed: 12006956]
31. Binion DG, Fu S, Kalathur S, et al. iNOS expression in human intestinal microvascular endothelial cells inhibits leukocyte adhesion. *Am J Physiol Gastrointest Liver Physiol.* 1998; 275:592.

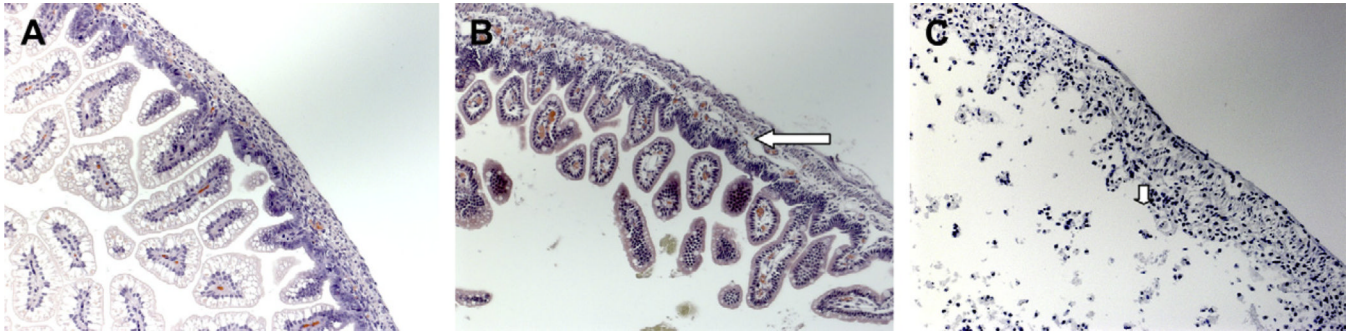


**FIG. 1.** Terminal ileum H and E sections from control pups [(A) magnification  $\times 20$ ] showing intact villi and close approximation of mucosa to underlying layers. Experimental pup intestine reveals grade 2 NEC, [(B) magnification  $\times 20$ ] in the formula fed/hypoxia pups and grade 4, [(C) magnification  $\times 20$ ] in the formula fed/hypoxia/LPS pups. The long arrow highlights moderate submucosal separation in grade 2 NEC and the short arrow shows evidence of villous sloughing in grade 4 NEC.

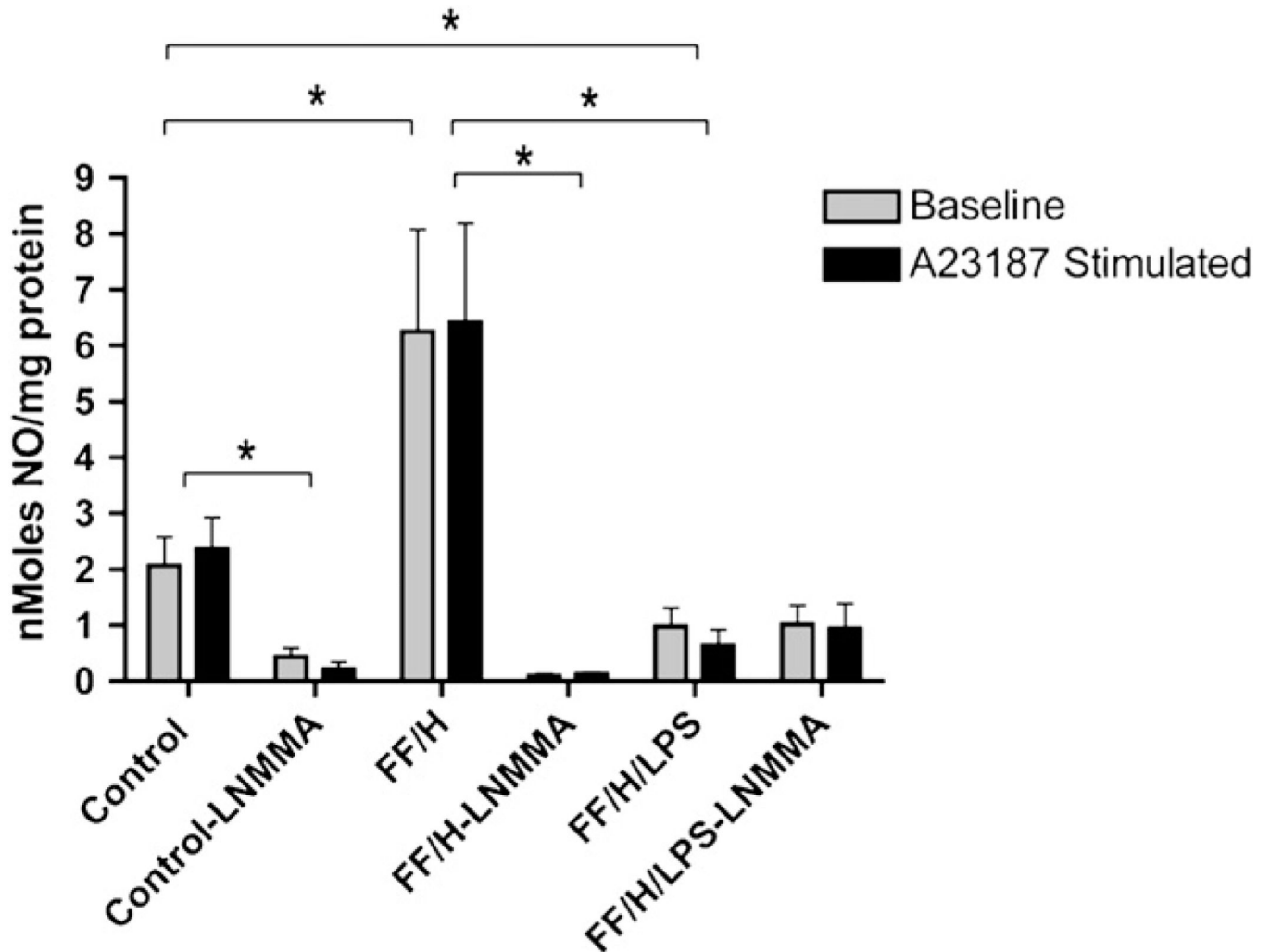


**FIG. 2.**

Mesenteric nitric oxide production. Nitric oxide production at baseline and following A23187 stimulation in control, formula fed/hypoxia (FF/H), and formula fed/hypoxia/LPS (FF/H/LPS) pups with and without NOS inhibitor L-NMMA. Error bars represent standard error of the mean (SEM) and  $P \leq 0.05$  are indicated with an asterisk (\*).

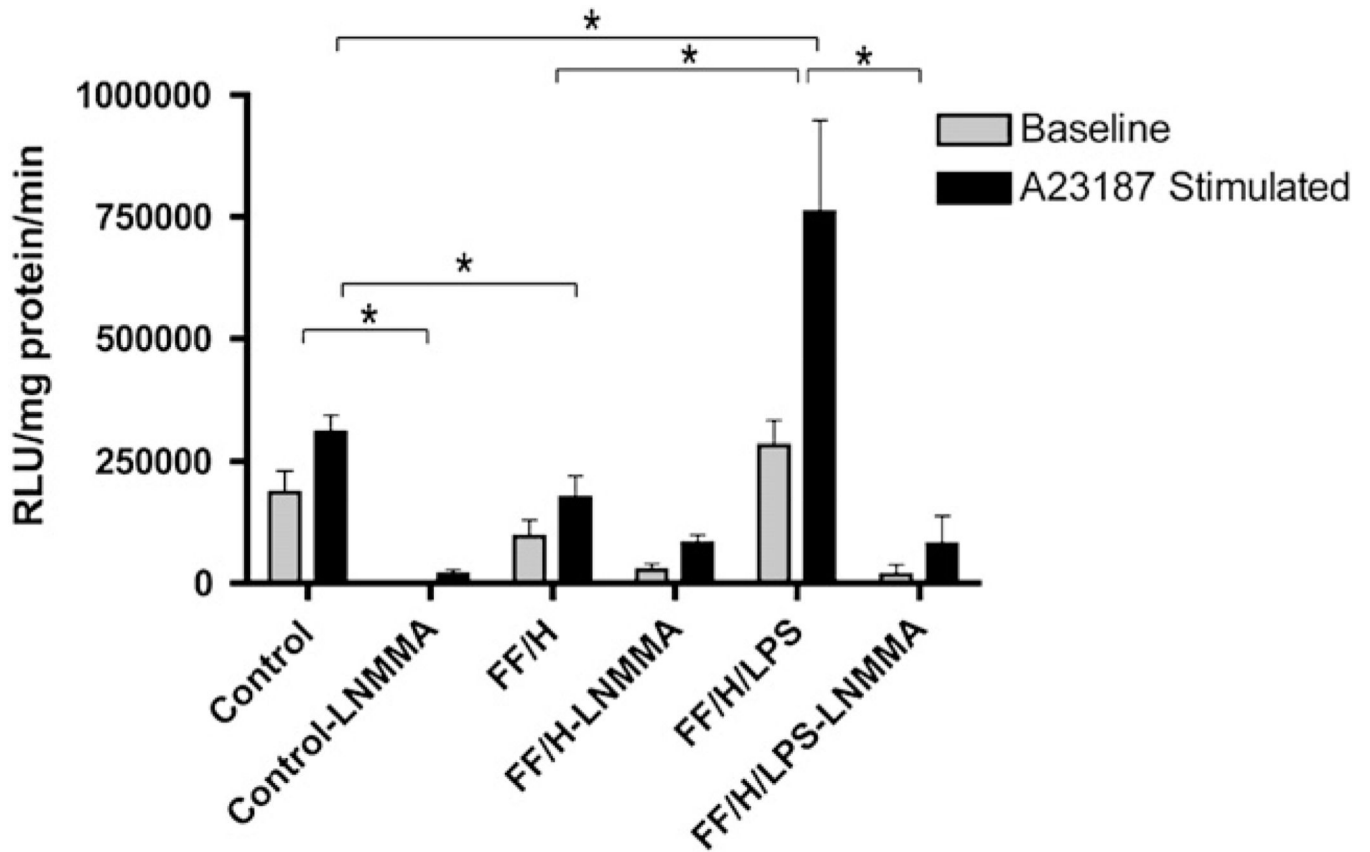


**FIG. 3.** Mesenteric superoxide production. Superoxide production at baseline and following A23187 stimulation in control, formula fed/hypoxia (FF/H), and formula fed/hypoxia/LPS (FF/H/LPS) pups with and without NOS inhibitor L-NMMA. Error bars represent standard error of the mean (SEM) and  $P \leq 0.05$  are indicated with an asterisk (\*).

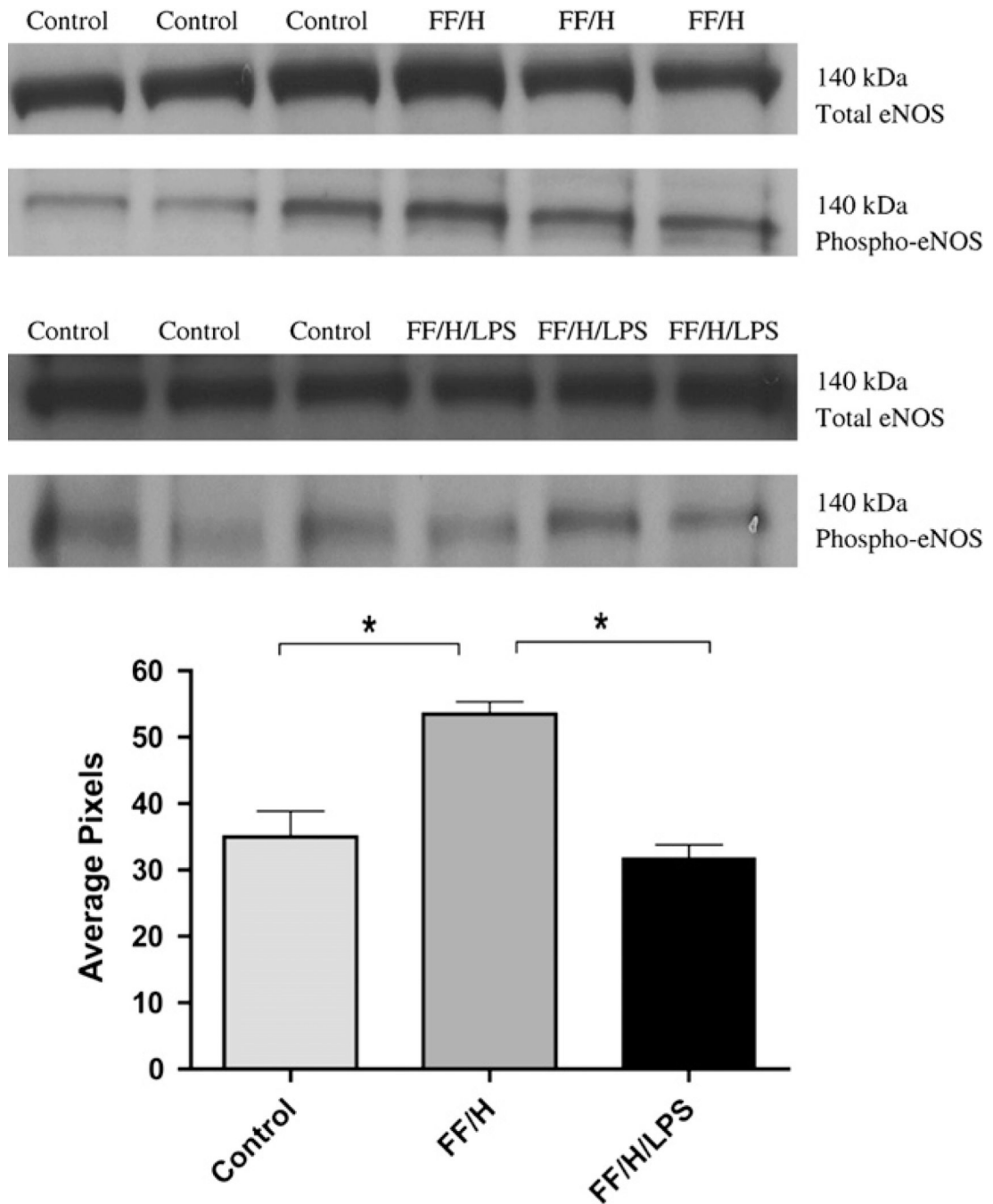


**FIG. 4.** eNOS and phospho-eNOS expression. Western blot band densities for total eNOS and phospho-eNOS in control versus formula fed/hypoxia (FF/H) pups and in control *versus* formula fed/hypoxia/LPS (FF/H/LPS) pups, molecular weights = 140 kDa. Densitometry data (mean pixels) for phospho-eNOS are shown graphically,  $n = 6$  for the control group and  $n = 3$  for both FF/H and FF/H/LPS groups. Error bars represent standard error of the mean (SEM) and  $P = 0.05$  are indicated with an asterisk (\*).



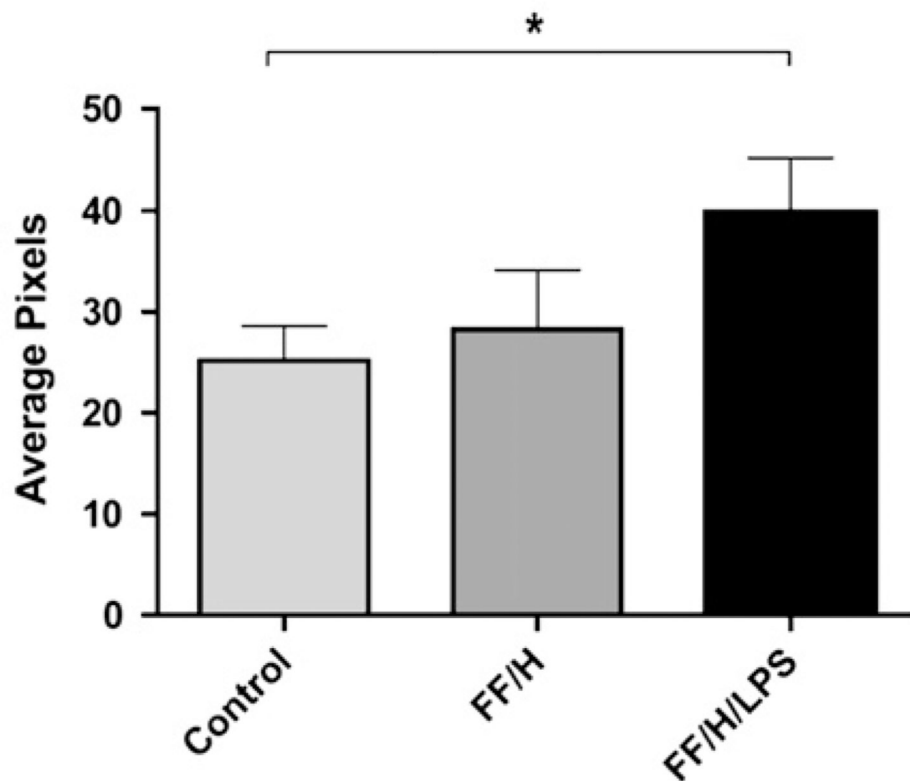
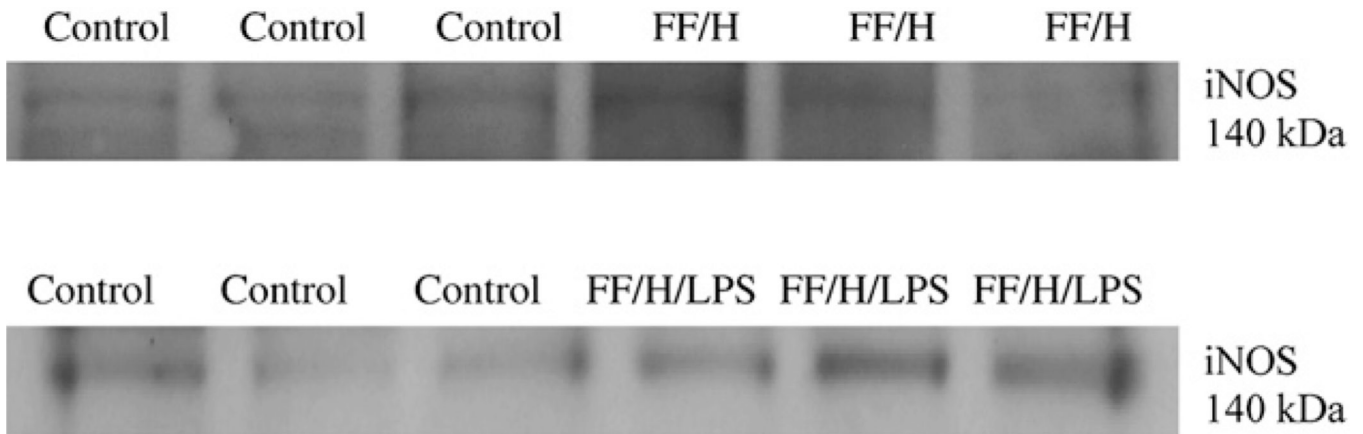


**FIG. 5.** iNOS expression. Western blot band densities for iNOS in control versus formula fed/hypoxia (FF/H) pups and in control *versus* formula fed/hypoxia/LPS (FF/H/LPS) pups, molecular weight = 140 kDa. Densitometry data (mean pixels) are shown graphically,  $n = 6$  for the control group and  $n = 3$  for both FF/H and FF/H/LPS groups. Error bars represent standard error of the mean (SEM) and  $P \leq 0.05$  are indicated with an asterisk (\*).

**TABLE 1**

Histology Grading Scale Used to Grade Degree of Intestinal Injury in Resected Terminal Ileum Specimens from Experimental NEC and Control Pups

<b>Grade</b>	<b>Histologic findings</b>
1	Mild submucosal and/or lamina propria separation
2	Moderate submucosal and/or lamina propria separation and/or edema in submucosa and/or muscular layers
3	Severe submucosal and/or lamina propria separation and/or edema in submucosal and muscular layers and regional villous sloughing
4	Necrosis, loss of villi

TABLE 2

Overall Representation of 14 Litters of Pups Used for Our Experiments

Litter	Total no. pups	Control	FF/hypoxia	FF/hypoxia/LPS	Mortality	Total pups studied
1	12	6	6	-	0	12
2	17	9	8	-	2	15
3	13	6	7	-	0	13
4	12	6	6	-	0	12
5	13	6	7	-	6	7
6	12	6	6	-	0	12
7	14	7	7	-	2	12
8	13	6	-	7	3	10
9	15	5	5	5	6	9
10	16	6	10	-	0	16
11	12	4	-	8	0	12
12	15	6	-	9	0	15
13	14	6	-	8	0	14
14	13	5	4	4	3	10
Total	191	84	66	41	22	171